

Serveur Académique Lausannois SERVAL serval.unil.ch

Author Manuscript

Faculty of Biology and Medicine Publication

This paper has been peer-reviewed but does not include the final publisher proof-corrections or journal pagination.

Published in final edited form as:

Title: Deficiency in monocarboxylate transporter 1 (MCT1) in mice delays regeneration of peripheral nerves following sciatic nerve crush.

Authors: Morrison BM, Tsingalia A, Vidensky S, Lee Y, Jin L, Farah MH, Lengacher S, Magistretti PJ, Pellerin L, Rothstein JD

Journal: Experimental neurology

Year: 2015 Jan

Volume: 263

Pages: 325-38

DOI: [10.1016/j.expneurol.2014.10.018](https://doi.org/10.1016/j.expneurol.2014.10.018)

In the absence of a copyright statement, users should assume that standard copyright protection applies, unless the article contains an explicit statement to the contrary. In case of doubt, contact the journal publisher to verify the copyright status of an article.

Published in final edited form as:

Exp Neurol. 2015 January ; 263: 325–338. doi:10.1016/j.expneurol.2014.10.018.

Deficiency in Monocarboxylate Transporter 1 (MCT1) in Mice Delays Regeneration of Peripheral Nerves following Sciatic Nerve Crush

Brett M. Morrison^a, Akivaga Tsingalia^a, Svetlana Vidensky^b, Youngjin Lee^b, Lin Jin^b, Mohamed H. Farah^a, Sylvain Lengacher^c, Pierre J. Magistretti^d, Luc Pellerin^e, and Jeffrey D. Rothstein^b

Brett M. Morrison: bmmorris7@jhmi.edu; Svetlana Vidensky: sylvain.lengacher@epfl.ch; Pierre J. Magistretti: pierre.magistretti@epfl.ch; Luc Pellerin: luc.pellerin@unil.ch; Jeffrey D. Rothstein: rothstein@jhmi.edu

^aDepartment of Neurology, School of Medicine, The Johns Hopkins University, 855 North Wolfe Street, Baltimore MD 21205 ^bBrain Science Institute and Department of Neurology, School of Medicine, The Johns Hopkins University, 855 North Wolfe Street, Baltimore MD 21205

^cLaboratory of Neuroenergetics and Cellular Dynamics, Ecole Polytechnique Federale de Lausanne, Lausanne, Switzerland ^dDivision of Biological and Environmental Sciences and Engineering, KAUST, Thuwal, Saudi Arabia and Brain Mind Institute, Ecole Polytechnique Federale de Lausanne, SV2511, Station 19, CH-1015, Lausanne, Switzerland ^eDepartment of Fundamental Neurosciences, University of Lausanne, 7 Rue du Bugnon, 1005 Lausanne, Switzerland

Abstract

Peripheral nerve regeneration following injury occurs spontaneously, but many of the processes require metabolic energy. The mechanism of energy supply to axons has not previously been determined. In the central nervous system, monocarboxylate transporter 1 (MCT1), expressed in oligodendroglia, is critical for supplying lactate or other energy metabolites to axons. In the current study, MCT1 is shown to localize within the peripheral nervous system to perineurial cells, dorsal root ganglion neurons, and Schwann cells by MCT1 immunofluorescence and MCT1 tdTomato BAC reporter mice. To investigate whether MCT1 is necessary for peripheral nerve regeneration, sciatic nerves in MCT1 heterozygous null mice are crushed and peripheral nerve regeneration quantified electrophysiologically and anatomically. Compound muscle action potential (CMAP) recovery is delayed from a median of 21 days in wild-type mice to greater than 38 days in MCT1 heterozygote null mice. In fact, half of the MCT1 heterozygote null mice have no recovery of CMAP at 42 days, while all of the wild-type mice recovered. In addition, muscle fibers remain 40% more atrophic and neuromuscular junctions 40% more denervated at 42 days

© 2014 Elsevier Inc. All rights reserved.

CORRESPONDING AUTHOR: Brett M. Morrison M.D., Ph.D., 855 North Wolfe Street, Rangos 248, The Johns Hopkins University, Baltimore MD 21205, bmmorris7@jhmi.edu, TEL: 410-502-0796, FAX: 410-502-5459.

Publisher's Disclaimer: This is a PDF file of an unedited manuscript that has been accepted for publication. As a service to our customers we are providing this early version of the manuscript. The manuscript will undergo copyediting, typesetting, and review of the resulting proof before it is published in its final citable form. Please note that during the production process errors may be discovered which could affect the content, and all legal disclaimers that apply to the journal pertain.

post-crush in the MCT1 heterozygote null mice than wild-type mice. The delay in nerve regeneration is not only in motor axons, as the number of regenerated axons in the sural sensory nerve of MCT1 heterozygote null mice at 4 weeks and tibial mixed sensory and motor nerve at 3 weeks is also significantly reduced compared to wild-type mice. This delay in regeneration may be partly through failed Schwann cell function, as there is reduced early phagocytosis of myelin debris and remyelination of axon segments. These data for the first time demonstrate that MCT1 is critical for regeneration of both sensory and motor axons in mice following sciatic nerve crush.

Keywords

monocarboxylate transporter; metabolism; regeneration; peripheral nerve; nerve crush; perineurial cell; Schwann cell; dorsal root ganglion; axon; electron microscopy

INTRODUCTION

Peripheral nerve regeneration following injury occurs spontaneously in the peripheral nervous system (PNS) through an orchestrated series of events initiated by Wallerian degeneration. The cellular mechanisms of Wallerian degeneration involve multiple cell types, including Schwann cells, perineurial cells (also termed fibroblasts or glia), macrophages, and neurons (Zochodne 2012). These cells downregulate some genes, particularly those associated with synaptic transmission, while upregulating others, including those typically associated with development (Scherer, Wang et al. 1994; Parmantier, Lynn et al. 1999; Mueller, Leonhard et al. 2003; Hunt, Hossain-Ibrahim et al. 2004; Gaudet, Popovich et al. 2011; Allodi, Udina et al. 2012; Blackmore 2012; Sulaiman and Gordon 2013). Many of these processes, including cell proliferation and gene activation, require metabolic energy. Despite this, little is known of the pathway for energy supply to peripheral nerves. Recent publications in the central nervous system (CNS) have suggested that monocarboxylate transporters (MCTs), particularly the oligodendroglial transporter MCT1 (SLC16A1), are critically important for supplying lactate to CNS axons (Funfschilling, Supplie et al. 2012; Lee, Morrison et al. 2012). In this study, we will investigate the dependence of peripheral nerves on MCT1 function.

Though originally thought to be a waste product of metabolism, evidence over the last few decades has established that lactate can be utilized as metabolic energy throughout the body (Gladden 2004). Intercellular lactate shuttles, in which a highly glycolytic cell produces lactate and transports it extracellularly through MCTs where it can be imported into adjacent cells that utilizes lactate for oxidative metabolism, have been found in muscle (Juel and Halestrap 1999) and the CNS (Pellerin, Pellegrini et al. 1998; Magistretti and Pellerin 1999; Magistretti and Pellerin 2000; Funfschilling, Supplie et al. 2012; Lee, Morrison et al. 2012). MCTs are extracellular membrane channels that transport lactate, pyruvate and ketone bodies, along with protons, down their concentration gradient across membranes (Garcia, Goldstein et al. 1994). MCT1-4 have been shown to transport monocarboxylates (see (Pellerin, Bergersen et al. 2005) for review). Of these transporters, only MCT1 has thus far been localized to the peripheral nerve, being localized to the perineurium surrounding nerve fascicles (Takebe, Nio-Kobayashi et al. 2008).

Perineurial cells, which form the layers of the perineurium (Du Plessis, Mouton et al. 1996), are connected by tight junctions and surrounded by basal lamina, thus making this layer restrictive to solutes from the blood and a primary component of the blood-nerve barrier (Akert, Sandri et al. 1976; Ghabriel, Jennings et al. 1989; Tserentsoodol, Shin et al. 1999). In addition to MCT1, perineurial cells also express the high-affinity glucose transporter, GLUT1, suggesting that perineurial cells may have an important metabolic function (Tserentsoodol, Shin et al. 1999; Takebe, Nio-Kobayashi et al. 2008). This metabolic role of perineurial cells may be particularly important in nerve growth, as recent studies from zebrafish have shown that these cells are necessary for peripheral nerve development and regeneration following injury (Kucenas, Takada et al. 2008; Binari, Lewis et al. 2013; Lewis and Kucenas 2014).

Direct evidence that peripheral nerves utilize lactate as metabolic energy *in vivo* is, thus far, lacking, but the dependence of axons on lactate has been conclusively demonstrated *ex vivo* in sciatic nerve explants (Brown, Evans et al. 2012). In this model system, application of glucose induces the production and release of lactate, and action potentials are reduced by blocking MCTs and subsequently restored by application of exogenous lactate. We postulate that peripheral nerves *in vivo* are also dependent on lactate, particularly during regeneration when they have their greatest requirement for energy. In this paper, we investigate the dependence of peripheral nerve regeneration on MCT1 by evaluating regrowth of sciatic nerve axons following nerve crush in MCT1 heterozygous null (MCT1 Het) mice.

METHODS

Animals

All mouse breeding and protocols were approved by the Johns Hopkins IACUC. Breeding colonies of MCT1 Het mice, obtained from Luc Pellerin and Pierre Magistretti, and BAC MCT1 tdTomato reporter mice (MCT1 Rep), previously described (Lee, Morrison et al. 2012), were maintained at Johns Hopkins University. MCT1 Het and MCT1 Rep mice were both on a C57Bl6 background. Proteolipid protein (PLP) eGFP reporter mice (Mallon, Shick et al. 2002), provided by Dr. Dwight Bergles, were on a B6/SJL mixed background.

Sciatic Nerve Crush

For nerve crush, 90–110 day old male transgenic (i.e., MCT1 Het null, BAC MCT1 tdTomato reporter, or PLP-GFP reporter) or litter-mate wild-type mice were anesthetized with 2% isoflurane/oxygen, lateral thigh shaved, and a 1 cm incision in the skin made over the lateral femur, as published previously (Ma, Omura et al. 2011). The muscle layers were split with blunt scissors, the sciatic nerve localized and crushed with a ultra-fine, smooth, straight hemostat (tip width 0.6 mm/ Fine Science Tools) for 20 seconds. The skin incision was closed with surgical staples and animals allowed to recover on a warming blanket. At various time points following nerve crush, mice were anesthetized with chloral hydrate, perfused, either with saline or 4% paraformaldehyde, and dissected for dorsal root ganglia (DRG), spinal cord, sciatic nerve (both proximal and distal to crush zone), sural nerve, tibial nerve, and/or muscle. Mice were perfused with saline when isolating mRNA or protein to wash out red blood cells that express high amounts of MCT1 (Dubinsky and Racker 1978;

Garcia, Brown et al. 1995). The investigator performing the surgeries was blinded to the genotype of the mice.

Muscle histology and neuromuscular junction quantification

In one cohort of WT and MCT1 Het mice, mice were anesthetized by an overdose of chloral hydrate and sacrificed by cervical dislocation (without transcardial perfusion) 6 weeks following sciatic nerve crush. Gastrocnemius muscles ipsilateral and contralateral to sciatic nerve crush were dissected, weighed, and either partly embedded in tragacanth and quick frozen in dry-ice cooled 2-methylbutane (for muscle histology) or cryoprotected in 25% sucrose, stretched and frozen in O.C.T. Tissue Tek compound (Fisher; for neuromuscular junction (NMJ) staining). For histology, gastrocnemius muscle sections (20 μ m) were cut transversely on a cryostat and processed with hematoxylin and eosin. For NMJ staining, gastrocnemius muscle sections (40 μ m) were cut longitudinally onto slides with a cryostat, incubated with 4% paraformaldehyde for 20 minutes, washed in PBS, blocked in 5% normal goat serum (in PBS with 0.3% Triton-X) and then incubated in primary antibody to synapsin (1:1000; R and D systems) for 2 days at 4°C. Following washes with PBS, the slides were then incubated simultaneously with biotinylated anti-rabbit secondary antibody (1:200; Vector Laboratories) and tetramethyl rhodamine-conjugated α -bungarotoxin (1:50; Life Technologies) for two hours at room temperature. Finally, slides were washed in PBS, incubated in Streptavidin conjugated to Alexa-Fluor 488 (1:1000; Invitrogen) for 1 hour and coverslipped with Prolong Gold (Life Technologies). Quantification of NMJ staining (double-labelled or innervated post-synaptic NMJs versus total post-synaptic NMJs) was completed manually on a Nikon E800 fluorescence microscope by an investigator blinded to the animals' genotype.

Electrophysiology

Prior to and 2 weeks following nerve crush, mice were evaluated for recovery of compound muscle action potentials (CMAPs) and conduction velocities biweekly through 6 weeks post-crush. These were completed by inserting stimulating electrodes in the sciatic notch in the vicinity of the proximal sciatic nerve, recording electrodes in the lateral plantar muscles of the foot pad, and a ground in the tail. All studies were completed with a Neurosoft-Evidence 3102 electromyograph. The stimulation parameters were a current of 10mA, duration of 0.05ms, and frequency of 1 Hz, and were designed to provide maximal stimulation of sciatic nerve. The investigator conducting the electrophysiology was blinded to the genotype of the mice throughout the study.

MCT1 Antibody Production

MCT1 antibody was produced for the Rothstein laboratory by Aves Labs (Tigard). Using proprietary software, the company identified an appropriate antigen (amino acids 477-493 at the C-terminus of the mouse protein) and conjugated this peptide to KLH. The antigen-KLH complex was used to immunize two chickens, the serum affinity purified and antibody production verified by ELISA. We further validated the antibody by Western blots of brain and sciatic nerves from wild-type and MCT1 Het mice and HEK cells expressing recombinant MCT1 protein (Suppl. Fig. 1A). Specificity of primary antibody was confirmed by blocking experiments (negative control) and recombinant MCT1 protein (positive

control). For the blocking experiments in Western blots, the primary antibody was incubated overnight at 4°C with or without antigen peptide (MCT1 amino acids 477-493; concentration 5-fold primary antibody) prior to application to membrane. For the immunofluorescence blocking experiments, the primary antibody was incubated for 1 hour at room temperature with or without antigen peptide (5-fold primary antibody) prior to application to sections. The positive control was HEK cells transfected with a lentivirus expressing the full MCT1 protein. These HEK cells were lysed and homogenized in TPER prior to running 50 µg of protein on Western blot.

Real-time RT PCR and Western blots

In dissected DRG or nerve, MCT1 mRNA was isolated by RNeasy Mini Kit (Qiagen), reverse transcribed to cDNA with High Capacity cDNA Reverse Transcription Kit (Applied Biosystems) and quantified by real-time RT PCR using Taqman probes (Applied Biosystems) for MCT1 relative to 18sRNA (DRG), actin, or peptidylprolyl isomerase A (PPIA; nerves) on a StepOne Plus RT-PCR System (Applied Biosystems). These housekeeping genes were chosen based on preliminary and/or published data (Girolami, Bouhy et al. 2010) that demonstrated gene expression to be stable following nerve crush. For Western blots, sciatic nerves, either proximal or distal to the crush, were homogenized in T-PER (Thermo Scientific) and run on Mini-Protean TGX Gels (10%; Bio-Rad) and transferred to nitrocellulose membranes (Bio-Rad). For all Western blots, 5 µg of sciatic nerves and 20 µg of brain were run on the gel. Membranes were incubated overnight with Rabbit polyclonal β-actin antibodies (AbCam; 1:3000) and visualized with Amersham ECL Reagent (GE Healthcare) on ImageQuant LAS 4000 (GE Healthcare). After visualizing β-actin, blots were stripped with Restore Western Blot Stripping Buffer (Thermo Scientific), reprobed overnight with chicken antibodies specific for mouse MCT1 (Rothstein laboratory; 1:300), and again visualized by ECL reagent, as described above.

Immunofluorescence and Electron Microscopy

Following transcardial perfusion with paraformaldehyde and dissection, as described above, tissue for immunofluorescence was post-fixed for 4 hours in 4% paraformaldehyde, cryoprotected in 20% sucrose and sectioned on a Leica CM1900 cryostat. Sections (20 µm thickness) were immunostained on slides for MCT1 (Rothstein lab; 1:500), S100 (Dako; 1:500), MAC2 (CedarLane; 1:1000), claudin-1 (Novus Biologicals; 1:200), non-phosphorylated or phosphorylated neurofilament (SMI32; Covance; 1:5000 or SMI31; Covance; 1:5000, respectively) either alone or in combination. Photomicrographs were taken on Zeiss LSM510 Meta confocal microscope. MAC2 immunofluorescent intensity was quantified by taking three randomly placed photomicrographs on the confocal microscope from each WT and MCT1 Het sciatic nerve post-crush, importing these images and quantifying in NIH Image J. For electron microscopy or semi-thin nerve histology, perfused nerves were post-fixed with 4% paraformaldehyde/2.5% glutaraldehyde for at least 3 days and embedded in Epon 812 resin. Embedded nerves were cut either semi-thin (1 µm) and stained with toluidine blue or thin (70 nm) and stained with citrate/uranyl acetate. Toluidine blue stained nerves were used for quantification of myelinated axon number, myelin debris, or g-ratios. For each of these histologic features, photomicrographs of sural nerves were taken on Nikon E800, imported and quantified manually with Zeiss AxioVision

4.8 software. G-ratios were calculated as the ratio of the diameter of axons divided by the diameter of myelin sheaths. If more than one fascicle was present in sample, the largest nerve fascicle was quantified in its entirety. The researcher quantifying the nerves was blinded to transgene status. EM photomicrographs were produced on a Zeiss Libra transmission electron microscope.

Statistics

Student's t-test was used to compare CMAP amplitudes (Figs. 2C, 3), axon number (Fig. 2A), conduction velocity (Fig. 2D), and MAC2 immunofluorescence intensity (Fig. 7B). Log rank test was used to compare groups in time to recover compound motor action potentials (CMAPs; Fig. 3A). One-way ANOVA with Sidak's multiple comparison tests was used to compare groups for MCT densitometry (Fig. 1C), CMAP amplitudes (Fig. 3C), muscle weights (Fig. 3G), neuromuscular junction (NMJ) innervation (Fig. 3H), G-ratios (Fig. 8C), and CMAP latencies (Fig. 8D). One-way ANOVA with Dunnett's multiple comparison tests was used for MCT1 densitometry and mRNA (Figs. 4B,C, 5H). Two-way ANOVA with Bonferroni post-test was used to compare groups for myelinated axon number (Fig. 3C, D) and myelin debris over time (Fig. 8).

RESULTS AND DISCUSSION

MCT1 is highly expressed in the PNS within perineurial cells, Schwann cells and DRG neurons

MCT1 mRNA expression in the sciatic nerve is approximately 200-fold greater than expression of MCT2 or MCT4, which are the other MCTs demonstrated to transport lactate in the nervous system (Fig. 1A). This is similar to the expression in the CNS, described previously (Lee, Morrison et al. 2012). MCT1 Het mice, published previously (Lee, Morrison et al. 2012; Lengacher, Nehiri-Sitayeb et al. 2013), have, as expected, a partial loss of MCT1 mRNA (Fig. 1A) and protein (Fig. 1B,C) in the brain and sciatic nerve. Complete knockout of MCT1 is embryonically lethal and therefore could not be evaluated in this study. MCT1 Het mice, which display injury to CNS axons by 6 months of age (Lee, Morrison et al. 2012), were used to evaluate the function of MCT1 in the PNS. Western blots were completed with a novel MCT1 antibody that, as expected, confirms the approximately 50% reduction of MCT1 protein in both brain and sciatic nerves of MCT1 Het mice (Fig. 1B,C). The specificity of the antibody is demonstrated by: 1) 50% reduction in Western blots of MCT1 Het mice (Fig. 1B,C); 2) selective immunostaining of a subset of myofibers, which are presumably type 1 myofibers based on prior publications, in the gastrocnemius muscle (Suppl. Fig. 1D)(McCullagh, Poole et al. 1996; Kobayashi 2004); 3) absence of immunoreactivity on Western blots or immunofluorescence of sciatic nerve after co-administration of antibody with blocking peptide (Suppl. Fig. 1A–F); and 4) specific labeling of MCT1 recombinant protein produced in HEK cells (Suppl. Fig. 1A; POS). By MCT1 immunofluorescence or the previously described MCT1 Rep mouse (Lee, Morrison et al. 2012), MCT1 in the sciatic nerve is strongly localized to perineurial cells (Fig. 1D–I; arrowheads). Perineurial cells also express Claudin-1 and co-localization with MCT1 Rep is found in the sciatic nerve (Fig. 1G–I). Though less intensely immunoreactive, Schwann cells, which are localized by S100 antibody, also co-localize MCT1 in the sciatic nerve (Fig.

1 J; arrows). The final cell type in the PNS that expresses MCT1, both in MCT1 Rep mice and WT mice immunostained with MCT1, is dorsal root ganglion (DRG) neurons (Fig. 1K, L). Though MCT1 appears to be expressed in peripheral nerve axons in MCT1 BAC mice (Fig. 1F), this may in fact be due to diffusion of tdTomato from DRG cell bodies into their axons, rather than true localization of the transporter within peripheral nerve axons. This is suggested by absence of co-localization of MCT1 immunoreactivity with phosphorylated neurofilaments, which label all sciatic nerve axons, in intact or crushed sciatic nerves (Suppl. Fig. 3A–D).

Using the MCT1 Rep mice and MCT1 immunofluorescence, our results confirm that MCT1 is localized to perineurial cells within peripheral nerves, as described previously (Takebe, Nio-Kobayashi et al. 2008). MCT1 Rep mice provide a sensitive tool for studying cellular expression of a gene of interest, and generally recapitulate both the localization and relative level of mRNA expression. This makes them ideal tools for studying molecules expressed at low levels both during normal physiologic function and following injury or degeneration. Given that the BAC reporter reflects mRNA expression, not protein, and that antibodies can be limited by their specificity and sensitivity, other components of peripheral nerves, such as axons, may express small amounts of stable MCT1 protein below the level of detection for our BAC reporter mouse and immunofluorescence techniques.

Peripheral nerves in MCT1 Het mice are structurally and functionally intact

Uninjured peripheral nerves in MCT1 Het mice are no different morphologically or electrophysiologically than age-matched wild-type (WT) mice. Sural nerves from 90–110 day old MCT1 Het mice, which is the age used for the subsequent experiments in this paper, show no evidence of axonal degeneration (Fig. 2). Axon number (Fig. 2A), axon diameter (Fig. 2B), and electrophysiologic characteristics, including compound muscle action potentials (CMAPs) and conduction velocity, in the sciatic nerve (Fig. 2C,D) are all unchanged compared to WT mice. Sural nerves from MCT1 Het mice demonstrate normal morphology by toluidine blue staining of semi-thin sections (Fig. 2J,K) and electron microscopy (Fig. 2L), compared to WT mice (Fig. 2G–I). Both myelinated and unmyelinated axons, localized to Remak bundles (Fig. 2I, L; arrows), are intact in MCT1 Het mice (Murinson, Hoffman et al. 2005). Additionally, there are no appreciable abnormalities in the perineurium or extracellular space in MCT1 Het mice (Fig. 2E,F), despite the reduction in MCT1 expression.

The absence of axon degeneration in peripheral nerves of MCT1 Het mice is quite different from CNS axons in the same mice, which display axonal swellings throughout white and gray matter from an absence of MCT1 on oligodendrocytes (Nave 2010; Lee, Morrison et al. 2012). The differences in susceptibility of PNS and CNS axons to reduced MCT1 expression suggests that PNS axons are not as dependent on MCT1 supplied energy substrates (e.g., lactate, pyruvate, ketone bodies) under normal physiologic conditions as their CNS counterparts. Of course, complete reduction of PNS MCT1, which is not possible with these null mice due to embryonic lethality, may uncover some dependence of peripheral axons. Given the lack of degeneration in peripheral axons, we next aimed to

uncover a role for MCT1 in repair and injury responses by examining whether MCT1 is required for peripheral nerve regeneration.

Peripheral nerve regeneration is delayed in MCT1 Het mice following sciatic nerve crush

Despite showing no abnormalities in uninjured nerves, MCT1 Het mice have markedly delayed recovery of both motor and sensory axons following proximal sciatic nerve crush. Sciatic nerves were crushed in order to reliably injure all of the axons, while allowing efficient regeneration to appropriate target tissues. Following unilateral sciatic nerve crush, mice were allowed to recover for up to 6 weeks. The time to recover measureable (> 0.2 mV) CMAPs (Fig. 3A; WT median 21 days, MCT1 Het median 38.5 days) and the average CMAP amplitude recovered over time (Fig. 3B) are significantly altered in MCT1 Het mice compared to WT mice. In addition to these electrophysiologic measures of motor nerve function, the number of regenerating myelinated axons from sural sensory and tibial mixed nerves, which are both distal to the crushed sciatic nerve, from MCT1 Het mice are also reduced (Fig. 3C–F). At 4 weeks following sciatic nerve crush in the sural nerve and 3 weeks in the tibial nerve, the number of myelinated axons is significantly reduced, though they both recover by 6 weeks post-crush (Fig. 3C, D). Representative photomicrographs from WT (Fig. 3E) and MCT1 Het (Fig. 3F) sural nerves 4 weeks following sciatic nerve crush demonstrate the reduction in myelinated axons stained with toluidine blue. The electrophysiologic and pathologic alterations in peripheral nerve regeneration are accompanied by persistent atrophy (Fig. 3G, I–L) and failed reinnervation (Fig. 3H, M–P) of denervated MCT1 Het muscle. Gastrocnemius muscle weights from MCT1 Het mice ipsilateral (Denervated) to sciatic nerve crush at 6 weeks are reduced compared to either MCT1 Het contralateral (Non-denervated) or WT ipsilateral muscle (Fig. 3G). This is also reflected by muscle fiber atrophy in hematoxylin and eosin stained muscle cross-sections of denervated MCT1 Het gastrocnemius (Fig. 3L) compared to denervated WT (Fig. 3K) or non-denervated WT or MCT1 Het (Fig. 3I, J) gastrocnemius. The muscle atrophy in MCT1 Het mice is due to persistent NMJ denervation at 6 weeks (Fig. 3H, P), a time point at which WT mice are fully re-innervated (Fig. 3H, O). WT muscle is fully re-innervated, despite incomplete recovery in CMAP amplitude by 6 weeks post-denervation. This is likely due to axonal sprouting of regenerated nerves at the muscle and enlarged motor units. Thus, by electrophysiology and pathology of nerves and muscles, MCT1 Het mice have a delay in both motor and sensory peripheral nerve regeneration. The delay in peripheral nerve regeneration following injury, but lack of abnormalities in uninjured peripheral nerves, suggests either that MCT1 is only important for peripheral nerves when energy need is highest, as during regeneration, or that there is a process specific to nerve regeneration that is dependent on MCT1. In order to begin evaluating the function of MCT1 in nerve regeneration, we evaluated MCT1 mRNA and protein expression in peripheral nerves and DRG by real-time RT PCR, Western blots, and MCT1 Rep mice.

Overall expression of MCT1 is reduced in peripheral nerves following sciatic nerve crush in WT mice

Intact and injured sciatic nerves from WT mice were isolated at 3, 7, and 14 days following sciatic nerve crush. Sciatic nerves were dissected into segments proximal or distal to the crush site and proteins isolated, while sciatic nerve segments from a second cohort of mice

proximal to the nerve crush, at the crush site, or distal to the crush were dissected and processed for mRNA. Expression of both MCT1 protein (Fig. 4A, B; Western blots) and mRNA (Fig. 4C; real-time RT PCR) are initially reduced in all nerve segments at 3 days post-crush relative to uncrushed nerves (***, $p < 0.001$; * $p < 0.05$). MCT1 protein returns to normal levels both proximal and distal to the crush by 7 days, while MCT1 mRNA remains reduced throughout the 14 days post-crush. All three major bands shown in Fig. 4A (doublet around 48kD and higher band around 60kD) were quantified for this analysis (see Suppl. Fig. 1G–I for full Western blots completed for this analysis), since all three bands are reduced in MCT1 Het mice (Fig. 1B; Suppl. Fig. 1A) and blocked by antigen peptide pre-incubation (Suppl. Fig. 1A). It should be noted that MCT1 mRNA or protein in crushed nerves is not elevated, compared to uncrushed nerves, at any time point in the first two weeks following injury.

MCT1 expression persists in perineurial cells, Schwann cells and DRG neurons following peripheral nerve injury

The pattern of cellular expression, evaluated in MCT1 Rep mice and WT mice by MCT1 immunofluorescence, is unchanged following sciatic nerve crush. Perineurial cells, labeled by claudin-1, express MCT1 in uncrushed MCT1 Rep mice (Fig. 5A). Following sciatic nerve crush, claudin-1-positive cells, presumed to be perineurial cells, continue to express MCT1 despite being internalized within the nerve fascicle (Fig. 5B, C; arrows). In addition to labeling in MCT1 Rep mice, claudin-1 positive perineurial cells in WT mice are also immunoreactive for MCT1 (Fig. 5D). As demonstrated previously, MCT1 is also expressed in DRG neurons (Fig. 1K, L). There is no qualitative or quantitative change in MCT1 mRNA expression following nerve crush in DRG, by MCT1 Rep mice (Fig. 5E–G) or real-time PCR of DRG from WT mice (Fig. 5H) at different time points following sciatic nerve crush. The final cell type in the PNS that expresses MCT1 is Schwann cells (Fig. 6). Schwann cells labeled by GFP (PLP Rep; green) in sciatic nerve from PLP-GFP transgenic mice co-localize with tdTomato from MCT1 Rep mice (red) in uncrushed (Fig. 6A, B) and 1 week crushed sciatic nerves from double transgenic mice (Fig. 6C, D). MCT1 immunoreactivity is also seen in Schwann cells, labelled with S100, in uncrushed (Fig. 6E–H) and 1 week crushed (Fig. 6I, J) sciatic nerves. Though immunoreactive, the intensity of MCT1 immunofluorescence in Schwann cells from uncrushed sciatic nerves (Fig. 6F–H; arrows) is clearly lower than perineurial cells (arrowheads). MCT1 immunofluorescence within Schwann cells appears to be increased following sciatic nerve crush (Fig. 6I, J), but this may reflect phagocytosis of MCT1 from other sources (i.e., perineurial cells or neurons), rather than true upregulation of MCT1 within Schwann cells. Macrophages and terminal Schwann cells are the final two cell-types evaluated, and there is no expression of MCT1 by MCT1 Rep mice in either. Macrophages, labelled with MAC2, do not co-localize with tdTomato from MCT1 Rep mice in intact or crushed sciatic nerves (Suppl. Fig. 3E–G). Additionally, terminal Schwann cells in the muscle, labeled with S100 (Suppl. Fig. 4A–E; green), do not co-localize with tdTomato (red) from MCT1 Rep mice in gastrocnemius muscles ipsilateral to intact or crushed sciatic nerves (1, 4, 7, or 42 days). Fluorescently-conjugated bungarotoxin (blue) was used to label the post-synaptic NMJ where the terminal Schwann cells are localized. From these experiments, it is clear that MCT1 is expressed in perineurial cells, DRG neurons, and Schwann cells in uninjured and crushed sciatic nerves

and that the overall level of peripheral nerve expression is initially lowered but rapidly returns to baseline after sciatic nerve crush.

The absence of clear upregulation of MCT1 by mRNA or protein in WT mice in one or more cell types following nerve injury makes conclusive determination of the exact cell types necessary for the function of MCT1 in peripheral nerve regeneration, and the mechanism by which MCT1 in these cells support nerve regeneration, more difficult. It does not, however, lessen the importance of MCT1 in peripheral nerve regeneration, since only a 50% decline in MCT1 dramatically delays regeneration. The initial downregulation of MCT1 expression suggests that developing therapies to increase MCT1 expression or activity could eventually be useful for accelerating peripheral nerve regeneration. In addition to being dependent on the speed of axon growth, nerve regeneration also requires robust and timely clearance of degenerating axons and myelin after nerve injury. This possible mechanism for failed regeneration was further investigated in MCT1 Het mice.

Myelin clearance is transiently disrupted in MCT1 Het mice

Delayed regeneration of peripheral nerves is not necessarily due to slowed axon regeneration, but can also be due to impaired clearance of myelin debris (Schafer, Fruttiger et al. 1996; Vargas, Watanabe et al. 2010; Farah, Pan et al. 2011; Painter, Brosius Lutz et al. 2014). As such, myelin clearance was investigated in MCT1 Het mice. Following sciatic nerve crush, there is a significant increase in the amount of myelin debris at one week in MCT1 Het mice compared to WT mice (Fig. 7A, C, D; arrows), which is cleared by two weeks post-crush (Fig. 7A, E, F; arrows). Reduced myelin clearance can be due to either attenuated macrophage activity or dysfunctional Schwann cells. To evaluate whether macrophages are sufficiently recruited to the injured axon and participate in myelin clearance, sciatic nerves from MCT1 Het and WT mice one week following nerve crush were immunostained for the macrophage marker, MAC2, and the intensity of immunofluorescence quantified by NIH Image J. MAC2 immunoreactivity is unchanged in MCT1 Het mice following nerve crush compared to WT mice (Fig. 7B, G–J).

Despite the normal MAC2 immunofluorescence, the increased amount of myelin debris in MCT1 Het mice soon after nerve crush suggests a deficiency in the breakdown of injured axons and myelin. Though this may contribute to the delay in peripheral nerve regeneration, the rapid clearance of myelin debris by 2 weeks post-crush makes it unlikely that this process is solely responsible for the delayed nerve regeneration. In addition to macrophages, the other cell type that participates in myelin/axon clearance is Schwann cells. In fact, Schwann cells have been shown to be the primary phagocytic cell in peripheral nerves within the first week after nerve injury (Stoll, Griffin et al. 1989; White, Toews et al. 1989; Liu, Yang et al. 1995; Hirata and Kawabuchi 2002). Thus, it is likely that reduced clearance of myelin debris in the first week actually reflects a defect in a critical Schwann cell function, rather than macrophage function. To investigate this further, we evaluated another function of Schwann cells, myelination, to determine if this is also dysfunctional in regenerating nerves from MCT1 Het mice.

Myelination of regenerating peripheral nerve axons is delayed in MCT1 Het mice

In order to evaluate myelination in regenerating peripheral nerves from MCT1 Het mice, sural and tibial nerves, which represent distal sensory and mixed (i.e., motor and sensory) nerves, respectively, were dissected from MCT1 Het and WT mice at 1–6 weeks following sciatic nerve crush. Nerve segments were embedded in resin and processed for toluidine blue staining or electron microscopy. Toluidine blue-stained sural nerves from MCT1 Het mice, dissected 6 weeks after sciatic nerve crush, have significantly greater g-ratio (indicating less myelination) than WT mice (Fig. 8A–C). This is also demonstrated electrophysiologically, as the CMAP latency, which reflects the state of myelination, is increased in regenerating MCT1 Het nerves following crush, but unchanged without crush (Fig. 8D). By electron microscopy, sural nerves isolated from MCT1 Het and WT mice 1 week following sciatic nerve crush both exhibit degenerating axons, though degenerated axons with maintained myelin, which is an earlier stage of myelin clearance, are seen more frequently in MCT1 Het mice (Fig. 8E, F). This is also seen in toluidine blue sections of the same nerves (Fig. 7C, D). Beginning in WT mice at 2 weeks post-crush, many regenerating axons are seen in the sural nerve (Figs. 7D, 8G), while few are seen in MCT1 Het mice at this time point (Fig. 7E, 8H). In fact, even at 3 weeks following sciatic nerve crush, sural (Fig. 8J) and tibial (Fig. 8L) nerves from MCT1 Het mice continue to have a multitude of unmyelinated or thinly myelinated axons, while only fully myelinated axons are seen in sural or tibial nerves from WT mice (Fig. 8I, K). Taken together, these results suggest that there is a delay in remyelination by Schwann cells in MCT1 Het mice.

Delayed remyelination and phagocytosis, which are both functions of Schwann cells, suggest that MCT1 is necessary for Schwann cell function. The exact mechanism by which MCT1 contributes to Schwann cell function is not addressed in this publication. Possible mechanisms include failure of energy supply to Schwann cells, perhaps through dysfunctional perineurial cells, or failure of metabolic energy import into Schwann cells through reduced MCT1 in Schwann cells. Future work will aim to distinguish between these two possibilities. Schwann cells have high metabolic needs, particularly in the setting of axon injury when they are responsible for clearing degenerating axons and myelin, providing cues for regrowing axons, and producing myelin components for the regenerating axons (Zochodne 2012). Our results suggest that lactate, or other energetic metabolites transported by MCT1, are important for meeting these additional metabolic needs.

Mechanisms for MCT1 in peripheral nerve regeneration

Our results demonstrate that MCT1 expression is important for peripheral nerve regeneration following injury. There are several possible mechanisms for this reduced regeneration, and our study is not able to definitively distinguish between them. Based on the observed localization of MCT1 in the PNS, downregulation of MCT1 in MCT1 Het mice could be impacting perineurial cells, Schwann cells or DRG neurons. Of these, MCT1 expression in perineurial and Schwann cells seem most likely to be responsible. Although MCT1 in DRG neurons could be important for nerve regeneration, likely through uptake and metabolic utilization of lactate, this mechanism would only explain the delay in nerve regeneration of sensory, and not motor, axons. Since regeneration of both are delayed and MCT1 is not expressed in motor neurons, as published previously (Lee, Morrison et al.

2012) and confirmed in our study by the absence of MCT1 tdTomato reporter in ventral roots (Suppl. Fig. 2), perineurial and Schwann cells are more likely the cellular substrate for the dependence of nerve regeneration on MCT1.

Perineurial cells are a major component of the blood-nerve barrier (Akert, Sandri et al. 1976; Ghabriel, Jennings et al. 1989; Tserentsoodol, Shin et al. 1999; Takebe, Nio-Kobayashi et al. 2008). In addition to expressing MCT1, they also express glucose transporters (i.e., Glut1) (Takebe, Nio-Kobayashi et al. 2008). Thus, perineurial cells have all the properties necessary to supply the endoneurium with energy metabolites. In this proposed mechanism, perineurial cells import glucose from the circulation through Glut1, metabolize it to lactate, and then transport lactate into the endoneurium through MCT1 where it may be used as metabolic fuel by Schwann cells and axons. This hypothesis is consistent with the growing literature that perineurial cells are crucial for developing, as well as recently regenerating, peripheral nerves (Kucenas, Takada et al. 2008; Binari, Lewis et al. 2013). Perineurial cells may also be important in peripheral neuropathies since they become inflamed and reduce their expression of connexins in diabetic rats (Pitre, Seifert et al. 2001), as well as develop pathologic changes in human neuropathies (Johnson, Brendel et al. 1981; King, Llewelyn et al. 1988; Hill and Williams 2004; Nolte, Hans et al. 2008). Our results provide, for the first time, a potential mechanism for this supportive role in developing and regenerating axons—namely, providing metabolic energy substrates, in the form of lactate, to Schwann cells and axons.

Schwann cells, which also express MCT1, are known to be key contributors to axon regeneration (Zochodne 2012) and could potentially utilize MCT1 to support peripheral nerve regeneration by either importing or exporting lactate. If an importer, intracellular lactate may help metabolically support Schwann cell function in normal physiology or repair of peripheral nerve injury. If an exporter, lactate produced by Schwann cells may support the energy needs of regenerating axons, such as has been demonstrated in the CNS (Lee, Morrison et al. 2012).

CONCLUSIONS

In summary, our results demonstrate for the first time that MCT1 expression is important for peripheral nerve regeneration following injury. MCT1 is expressed in perineurial cells, endoneurial Schwann cells, and DRG neurons, but not in terminal Schwann cells, endoneurial macrophages, or sciatic nerve axons. MCT1 Het mice, which express approximately 50% of WT MCT1, have delayed regeneration of peripheral nerves following sciatic nerve crush. The delay in regeneration occurs in motor nerves, as measured by recovery of CMAPs, muscle atrophy, and neuromuscular junction innervation, as well as sensory nerves measured by counts of sural nerve axons. Our findings suggest that the delay in axonal regeneration is accompanied by a delay or dysfunction of Schwann cells either due to reduced availability of endoneurial lactate (secondary to failed transport through the perineurium) or decreased uptake of lactate into Schwann cells (secondary to failed import). Future studies using cell-specific knockdown of MCT1 by genetic recombination (i.e., *LoxP*) will be exceptionally useful to further dissect the specific role for perineurial, DRG, and Schwann cell MCT1.

Supplementary Material

Refer to Web version on PubMed Central for supplementary material.

Acknowledgments

The authors would like to thank Dr. Rita Sattler for her helpful comments on the manuscript, Dr. Dwight Bergles for supplying the PLP-GFP transgenic reporter mice, Ms. Katelyn Russell for assistance with electrodiagnostic studies, and Carol Cooke and the Johns Hopkins Neurology Electron Microscopy Core for their assistance in processing, photographing, and analyzing electron microscopic images. Financial support was provided by the Muscular Dystrophy Association (B.M.M.), NIH-NS33958 (J.D.R.), and the Packard Center for ALS (J.D.R.).

Abbreviations

PNS	peripheral nervous system
CNS	central nervous system
MCT	monocarboxylate transporter
GLUT1	glucose transporter 1
DRG	dorsal root ganglion
PLP	proteolipid protein
NMJ	neuromuscular junction
CMAP	compound muscle action potential
PPIA	peptidylprolyl isomerase A or cyclophilin A
GAPDH	glyceraldehyde 3-phosphate dehydrogenase
WT	wild-type mice
MCT1 Het	MCT1 heterozygous null mice

References

- Akert K, Sandri C, et al. The fine structure of the perineural endothelium. *Cell Tissue Res.* 1976; 165(3):281–295. [PubMed: 1082372]
- Allodi I, Udina E, et al. Specificity of peripheral nerve regeneration: interactions at the axon level. *Prog Neurobiol.* 2012; 98(1):16–37. [PubMed: 22609046]
- Binari LA, Lewis GM, et al. Perineurial glia require Notch signaling during motor nerve development but not regeneration. *J Neurosci.* 2013; 33(10):4241–4252. [PubMed: 23467342]
- Blackmore MG. Molecular control of axon growth: insights from comparative gene profiling and high-throughput screening. *Int Rev Neurobiol.* 2012; 105:39–70. [PubMed: 23206595]
- Brown AM, Evans RD, et al. Schwann cell glycogen selectively supports myelinated axon function. *Ann Neurol.* 2012; 72(3):406–418. [PubMed: 23034913]
- Du Plessis DG, Mouton YM, et al. An ultrastructural study of the development of the chicken perineurial sheath. *J Anat.* 1996; 189(Pt 3):631–641. [PubMed: 8982839]
- Dubinsky WP, Racker E. The mechanism of lactate transport in human erythrocytes. *J Membr Biol.* 1978; 44(1):25–36. [PubMed: 32398]
- Farah MH, Pan BH, et al. Reduced BACE1 activity enhances clearance of myelin debris and regeneration of axons in the injured peripheral nervous system. *J Neurosci.* 2011; 31(15):5744–5754. [PubMed: 21490216]

- Funfschilling U, Supplie LM, et al. Glycolytic oligodendrocytes maintain myelin and long-term axonal integrity. *Nature*. 2012; 485(7399):517–521. [PubMed: 22622581]
- Garcia CK, Brown MS, et al. cDNA cloning of MCT2, a second monocarboxylate transporter expressed in different cells than MCT1. *J Biol Chem*. 1995; 270(4):1843–1849. [PubMed: 7829520]
- Garcia CK, Goldstein JL, et al. Molecular characterization of a membrane transporter for lactate, pyruvate, and other monocarboxylates: implications for the Cori cycle. *Cell*. 1994; 76(5):865–873. [PubMed: 8124722]
- Gaudet AD, Popovich PG, et al. Wallerian degeneration: gaining perspective on inflammatory events after peripheral nerve injury. *J Neuroinflammation*. 2011; 8:110. [PubMed: 21878126]
- Ghabriel MN, Jennings KH, et al. Diffusion barrier properties of the perineurium: an in vivo ionic lanthanum tracer study. *Anat Embryol (Berl)*. 1989; 180(3):237–242. [PubMed: 2596704]
- Girolami EI, Bouhy D, et al. Differential expression and potential role of SOCS1 and SOCS3 in Wallerian degeneration in injured peripheral nerve. *Exp Neurol*. 2010; 223(1):173–182. [PubMed: 19576891]
- Gladden LB. Lactate metabolism: a new paradigm for the third millennium. *J Physiol*. 2004; 558(Pt 1): 5–30. [PubMed: 15131240]
- Hill RE, Williams PE. Perineurial cell basement membrane thickening and myelinated nerve fibre loss in diabetic and nondiabetic peripheral nerve. *J Neurol Sci*. 2004; 217(2):157–163. [PubMed: 14706218]
- Hirata K, Kawabuchi M. Myelin phagocytosis by macrophages and nonmacrophages during Wallerian degeneration. *Microsc Res Tech*. 2002; 57(6):541–547. [PubMed: 12112437]
- Hunt D, Hossain-Ibrahim K, et al. ATF3 upregulation in glia during Wallerian degeneration: differential expression in peripheral nerves and CNS white matter. *BMC Neurosci*. 2004; 5:9. [PubMed: 15113454]
- Johnson PC, Brendel K, et al. Human diabetic perineurial cell basement membrane thickening. *Lab Invest*. 1981; 44(3):265–270. [PubMed: 7464050]
- Juel C, Halestrap AP. Lactate transport in skeletal muscle - role and regulation of the monocarboxylate transporter. *J Physiol*. 1999; 517(Pt 3):633–642. [PubMed: 10358105]
- King RH, Llewelyn JG, et al. Perineurial calcification. *Neuropathol Appl Neurobiol*. 1988; 14(2):105–123. [PubMed: 2840592]
- Kobayashi M. Fiber type-specific localization of monocarboxylate transporters MCT1 and MCT4 in rat skeletal muscle. *Kurume Med J*. 2004; 51(3–4):253–261. [PubMed: 15682832]
- Kucenas S, Takada N, et al. CNS-derived glia ensheath peripheral nerves and mediate motor root development. *Nat Neurosci*. 2008; 11(2):143–151. [PubMed: 18176560]
- Lee Y, Morrison BM, et al. Oligodendroglia metabolically support axons and contribute to neurodegeneration. *Nature*. 2012; 487:443–448. [PubMed: 22801498]
- Lengacher S, Nehiri-Sitayeb T, et al. Resistance to diet-induced obesity and associated metabolic perturbations in haploinsufficient monocarboxylate transporter 1 mice. *PLoS One*. 2013; 8(12):e82505. [PubMed: 24367518]
- Lewis GM, Kucenas S. Perineurial Glia Are Essential for Motor Axon Regrowth following Nerve Injury. *J Neurosci*. 2014; 34(38):12762–12777. [PubMed: 25232113]
- Liu HM, Yang LH, et al. Schwann cell properties: 3. C-fos expression, bFGF production, phagocytosis and proliferation during Wallerian degeneration. *J Neuropathol Exp Neurol*. 1995; 54(4):487–496. [PubMed: 7602323]
- Ma CH, Omura T, et al. Accelerating axonal growth promotes motor recovery after peripheral nerve injury in mice. *J Clin Invest*. 2011; 121(11):4332–4347. [PubMed: 21965333]
- Magistretti PJ, Pellerin L. Cellular mechanisms of brain energy metabolism and their relevance to functional brain imaging. *Philos Trans R Soc Lond B Biol Sci*. 1999; 354(1387):1155–1163. [PubMed: 10466143]
- Magistretti PJ, Pellerin L. The astrocyte-mediated coupling between synaptic activity and energy metabolism operates through volume transmission. *Prog Brain Res*. 2000; 125:229–240. [PubMed: 11098660]

- Mallon BS, Shick HE, et al. Proteolipid promoter activity distinguishes two populations of NG2-positive cells throughout neonatal cortical development. *J Neurosci*. 2002; 22(3):876–885. [PubMed: 11826117]
- McCullagh KJ, Poole RC, et al. Role of the lactate transporter (MCT1) in skeletal muscles. *Am J Physiol*. 1996; 271(1 Pt 1):E143–150. [PubMed: 8760092]
- Mueller M, Leonhard C, et al. Macrophage response to peripheral nerve injury: the quantitative contribution of resident and hematogenous macrophages. *Lab Invest*. 2003; 83(2):175–185. [PubMed: 12594233]
- Murinson BB, Hoffman PN, et al. C-fiber (Remak) bundles contain both isolectin B4-binding and calcitonin gene-related peptide-positive axons. *J Comp Neurol*. 2005; 484(4):392–402. [PubMed: 15770655]
- Nave KA. Myelination and support of axonal integrity by glia. *Nature*. 2010; 468(7321):244–252. [PubMed: 21068833]
- Nolte KW, Hans VJ, et al. Perineurial cells filled with collagen in ‘atypical’ Cogan’s syndrome. *Acta Neuropathol*. 2008; 115(5):589–596. [PubMed: 17885761]
- Painter MW, Brosius Lutz A, et al. Diminished schwann cell repair responses underlie age-associated impaired axonal regeneration. *Neuron*. 2014; 83(2):331–343. [PubMed: 25033179]
- Parmantier E, Lynn B, et al. Schwann cell-derived Desert hedgehog controls the development of peripheral nerve sheaths. *Neuron*. 1999; 23(4):713–724. [PubMed: 10482238]
- Pellerin L, Bergersen LH, et al. Cellular and subcellular distribution of monocarboxylate transporters in cultured brain cells and in the adult brain. *J Neurosci Res*. 2005; 79(1–2):55–64. [PubMed: 15573400]
- Pellerin L, Pellegrini G, et al. Evidence supporting the existence of an activity-dependent astrocyte-neuron lactate shuttle. *Dev Neurosci*. 1998; 20(4–5):291–299. [PubMed: 9778565]
- Pitre DA, Seifert JL, et al. Perineurium inflammation and altered connexin isoform expression in a rat model of diabetes related peripheral neuropathy. *Neurosci Lett*. 2001; 303(1):67–71. [PubMed: 11297825]
- Schafer M, Fruttiger M, et al. Disruption of the gene for the myelin-associated glycoprotein improves axonal regrowth along myelin in C57BL/Wjds mice. *Neuron*. 1996; 16(6):1107–1113. [PubMed: 8663987]
- Scherer SS, Wang DY, et al. Axons regulate Schwann cell expression of the POU transcription factor SCIP. *J Neurosci*. 1994; 14(4):1930–1942. [PubMed: 8158248]
- Stoll G, Griffin JW, et al. Wallerian degeneration in the peripheral nervous system: participation of both Schwann cells and macrophages in myelin degradation. *J Neurocytol*. 1989; 18(5):671–683. [PubMed: 2614485]
- Sulaiman W, Gordon T. Neurobiology of peripheral nerve injury, regeneration, and functional recovery: from bench top research to bedside application. *Ochsner J*. 2013; 13(1):100–108. [PubMed: 23531634]
- Takebe K, Nio-Kobayashi J, et al. Histochemical demonstration of a monocarboxylate transporter in the mouse perineurium with special reference to GLUT1. *Biomed Res*. 2008; 29(6):297–306. [PubMed: 19129673]
- Tserentsoodol N, Shin BC, et al. Immunolocalization of tight junction proteins, occludin and ZO-1, and glucose transporter GLUT1 in the cells of the blood-nerve barrier. *Arch Histol Cytol*. 1999; 62(5):459–469. [PubMed: 10678575]
- Vargas ME, Watanabe J, et al. Endogenous antibodies promote rapid myelin clearance and effective axon regeneration after nerve injury. *Proc Natl Acad Sci U S A*. 2010; 107(26):11993–11998. [PubMed: 20547838]
- White FV, Toews AD, et al. Lipid metabolism during early stages of Wallerian degeneration in the rat sciatic nerve. *J Neurochem*. 1989; 52(4):1085–1092. [PubMed: 2926390]
- Zochodne DW. The challenges and beauty of peripheral nerve regrowth. *J Peripher Nerv Syst*. 2012; 17(1):1–18. [PubMed: 22462663]

Highlights

1. MCT1 expressed in perineurial cells, Schwann cells and dorsal root ganglia neurons
2. Uninjured peripheral nerves are normal in MCT1 heterozygous null mice
3. Peripheral nerve regeneration attenuated in MCT1 heterozygous null mice
4. Schwann cells in MCT1 heterozygous null mice dysfunctional during regeneration

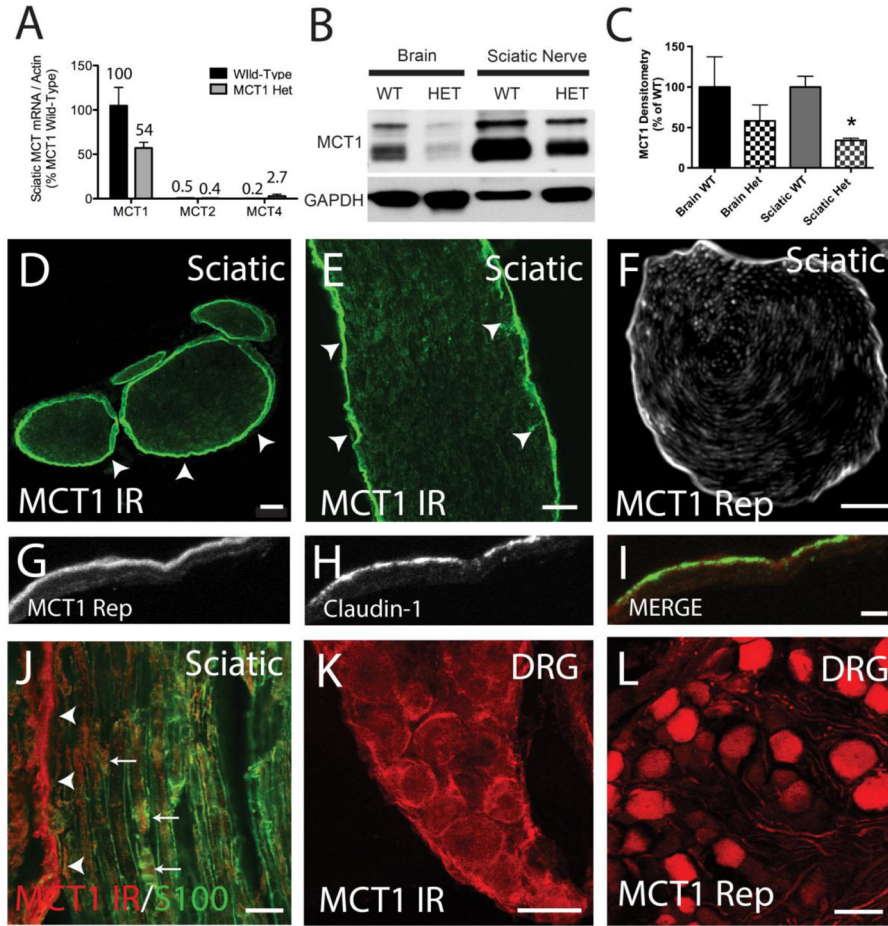


Figure 1. Localization of MCT1 in the peripheral nervous system

(A) MCT mRNA expression by real-time RT PCR in the sciatic nerves of wild-type (WT) and MCT1 heterozygous null (MCT1 Het) mice. All values are percentages relative to MCT1 mRNA in WT mice (n=3). Western blot (B) and densitometry quantification (C) of MCT1 protein in WT and MCT1 Het mice. MCT1 immunoreactivity (MCT1 IR) in cross-section (D) and longitudinal section (E) of sciatic nerve from WT mice alone or co-localized with Schwann cell marker, S100 (J). Perineurium (D–I; arrowheads) is strongly immunoreactive, though there is some co-localization with Schwann cells (J; arrows) in mouse peripheral nerves, as well (D, E scale bars 100 μ m; F scale bar 20 μ m). Identical to immunofluorescence, MCT1 BAC tdTomato reporter expression localizes primarily to the perineurium (F). Perineurial cells, labelled with claudin-1 immunofluorescence (green), also express tdTomato in MCT1 BAC reporter mice (G–I; red, scale bars 5 μ m). Dorsal root ganglion (DRG) neurons are immunoreactive for MCT1 (K) and positive for MCT1 BAC reporter (L; scale bars 50 μ m). Error bars reflect standard error of the means (S.E.M.).

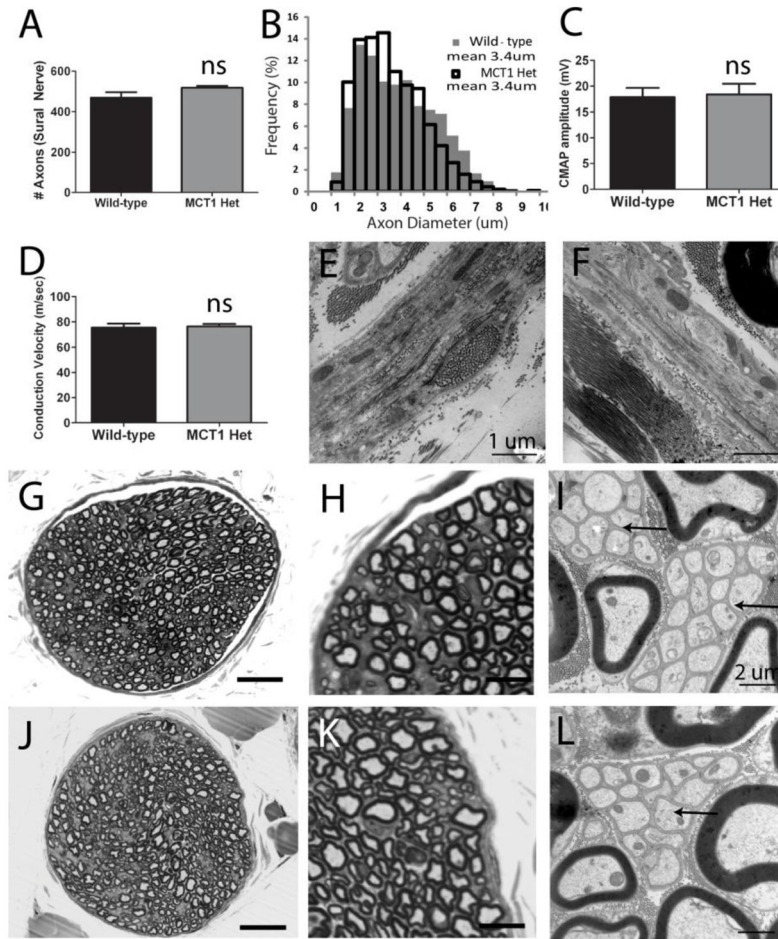


Figure 2. Morphology and electrophysiologic properties of nerves from MCT1 Heterozygous null (MCT1 Het) mice

Quantification of axon number (A) and axon diameter (B) in sural nerve from WT (n=6) and MCT1 Het (n=4) mice. Compound motor action potential (CMAP) amplitude (C) and conduction velocity (D) following sciatic nerve stimulation in WT (n=8) and MCT1 Het (n=7) mice. Perineurium in WT (E) and MCT1 Het (F) mice (scale bars 1 μm). Photomicrographs of wild type (G–I) and MCT1 Het (J–L) sural nerves processed for light (G, H, J, K; scale bars 100 μm G, J; 10 μm H, K) and electron (I, L; scale bars 2 μm) microscopy. Arrows indicate Remak bundles of unmyelinated axons in WT (I) and MCT1 Het (L) mice. All error bars reflect S.E.M.

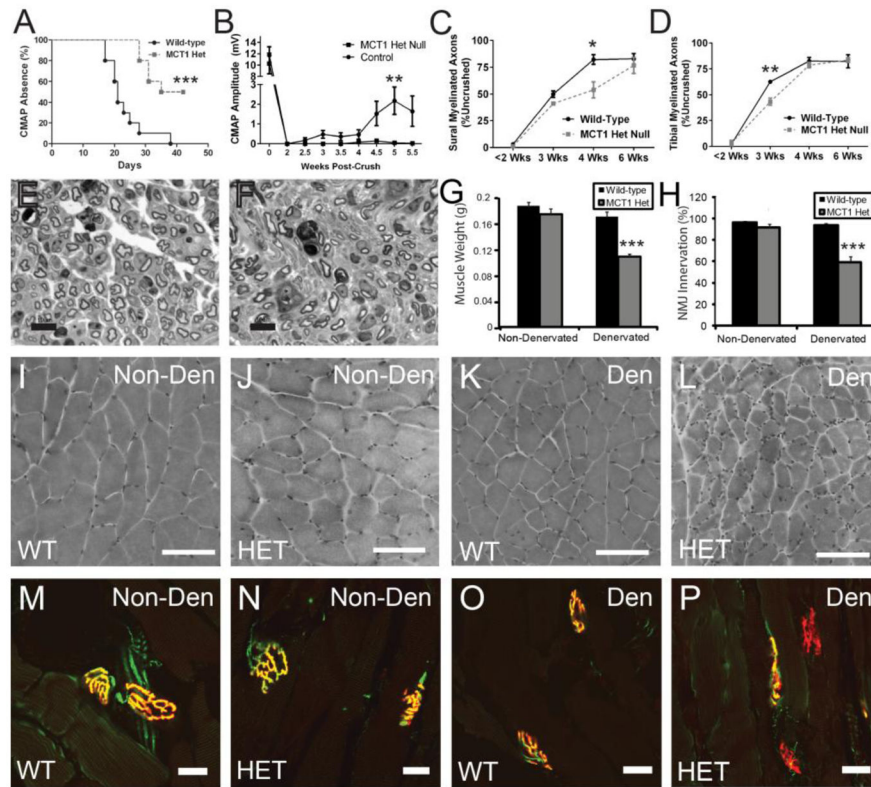


Figure 3. MCT1 heterozygous null (MCT1 Het) mice have delayed regeneration following sciatic nerve injury

(A) Time to recovery of compound motor action potentials (CMAPs) following sciatic nerve crush in MCT1 Het (HET; n=9) compared to WT (WT; n=10) mice (Kaplan-Meier curve).

(B) Mean CMAP amplitude of WT and Het mice pre-crush (time 0) and then from 2 to 5.5 weeks following sciatic nerve crush (n=10 each). If no CMAP amplitude was recordable, the value is counted as 0. Myelinated axon number in the sural nerve (C), which is a pure sensory nerve, and tibial nerve (D), which is a mixed motor and sensory nerve, displayed as percentage of axon number in uncrushed nerves, at less than 2 weeks (1 and 2 weeks combined; n=6 WT, n=5 Het), 3 weeks (n=2 WT, n=2 Het), 4 weeks (n=3 WT, n=3 Het), and 6 weeks (n=5 WT, n=5 Het) post-sciatic nerve crush.

Sural nerve 4 weeks following sciatic nerve crush in WT (E) and Het (F) mice (scale bars 10 μ m). Quantification of gastrocnemius muscle weights (G; n=12 WT, n=10 Het) and NMJ innervation (H; n=4 WT, n=5 Het) in non-denervated and 6 weeks denervated WT and MCT1 Het mice.

Photomicrographs of hematoxylin and eosin (I–L; scale bars 100 μ m) and NMJ (M–P; scale bars 20 μ m) stained gastrocnemius muscles from non-denervated (Non-Den) WT (I, M) and MCT1 Het (J, N) mice or 6 weeks following denervation (Den) in WT (K, O) and MCT1 Het (L, P) mice. For NMJ staining, presynaptic terminal labeled with synapsin (green) and post-synaptic motor endplate labeled with tetra-rhodamine-conjugated bungarotoxin (red). All error bars reflect S.E.M. * p<0.05, ** p<0.01, *** p<0.001

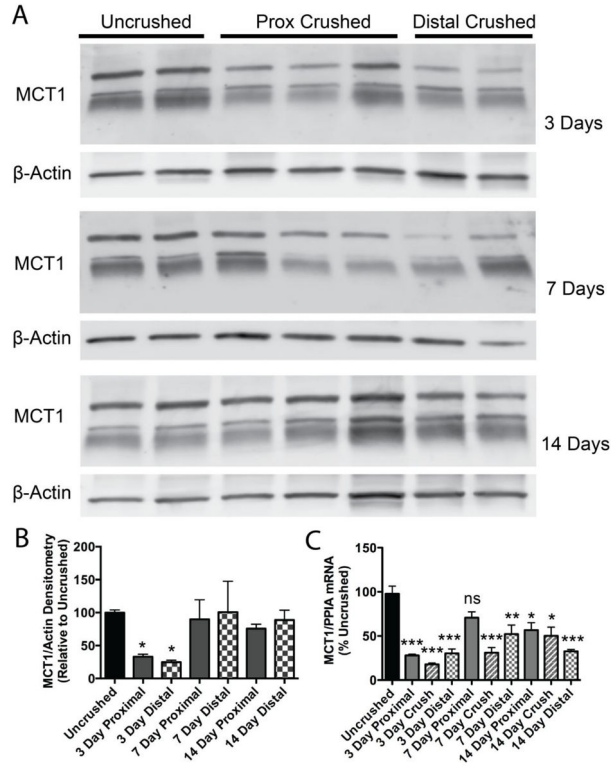


Figure 4. MCT1 mRNA and protein quantification following sciatic nerve crush

Western blot (A) and densitometry (B) for MCT1, relative to β -actin reference protein, in sciatic nerves that are uncrushed (n=15) or 3 (n=6), 7 (n=6), or 14 (n=6) days following crush (both proximal and distal to crush site) from WT mice. Both the lower doublet and upper band were quantified for densitometry. MCT1 mRNA (C), by real-time RT PCR relative to PPIA reference gene, in sciatic nerves that are uncrushed (n=12) or 3, 7, or 14 days (n=4 each) following crush (proximal to crush, crush zone, or distal to crush) in WT mice. All graphs are shown as percentage of uncrushed. * p<0.05, ** p<0.01, *** p<0.001, relative to uncrushed nerves and controlled for multiple comparisons. All error bars reflect S.E.M.

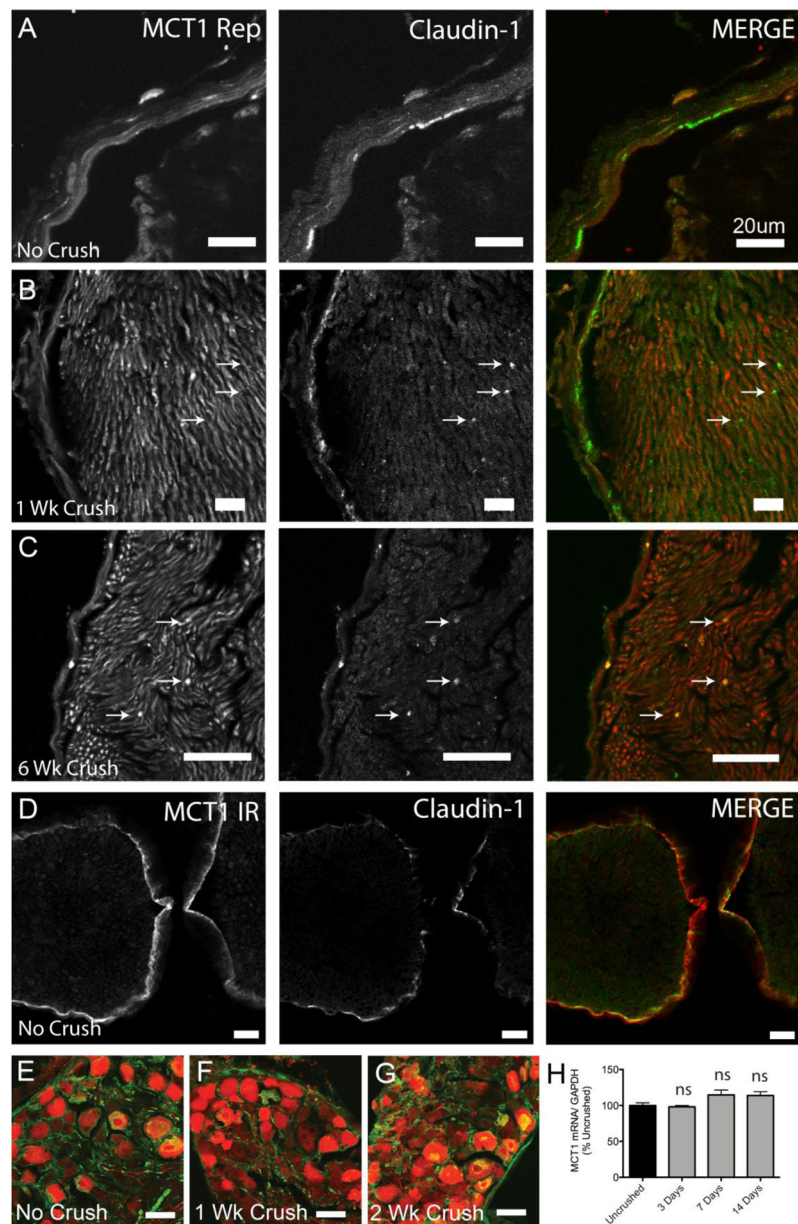


Figure 5. MCT1 expression in perineurial cells of intact and injured sciatic nerves
 Uncrushed (A), 1 (B) and 6 (C) weeks post-crush sciatic nerves from MCT1 BAC tdTomato reporter (red) immunolabeled with the perineurial cell marker, claudin-1 (green; indicated by arrows). Uncrushed sciatic nerves from WT mice (D) immunostained for MCT1 (MCT1ir; red) and Claudin-1 (green; Scale bars 20 μ m). DRG ipsilateral to uncrushed (E), 1 (F) and 2 (G) weeks crushed sciatic nerves from tdTomato MCT1 reporter mice (red) immunostained for non-phosphorylated neurofilament (green; scale bars E–G 50 μ m). MCT1 mRNA quantification (H), by real-time RT PCR, of DRG following sciatic nerve crush (n=9 uncrushed, n=3 for each time point post-crush). All error bars reflect S.E.M.

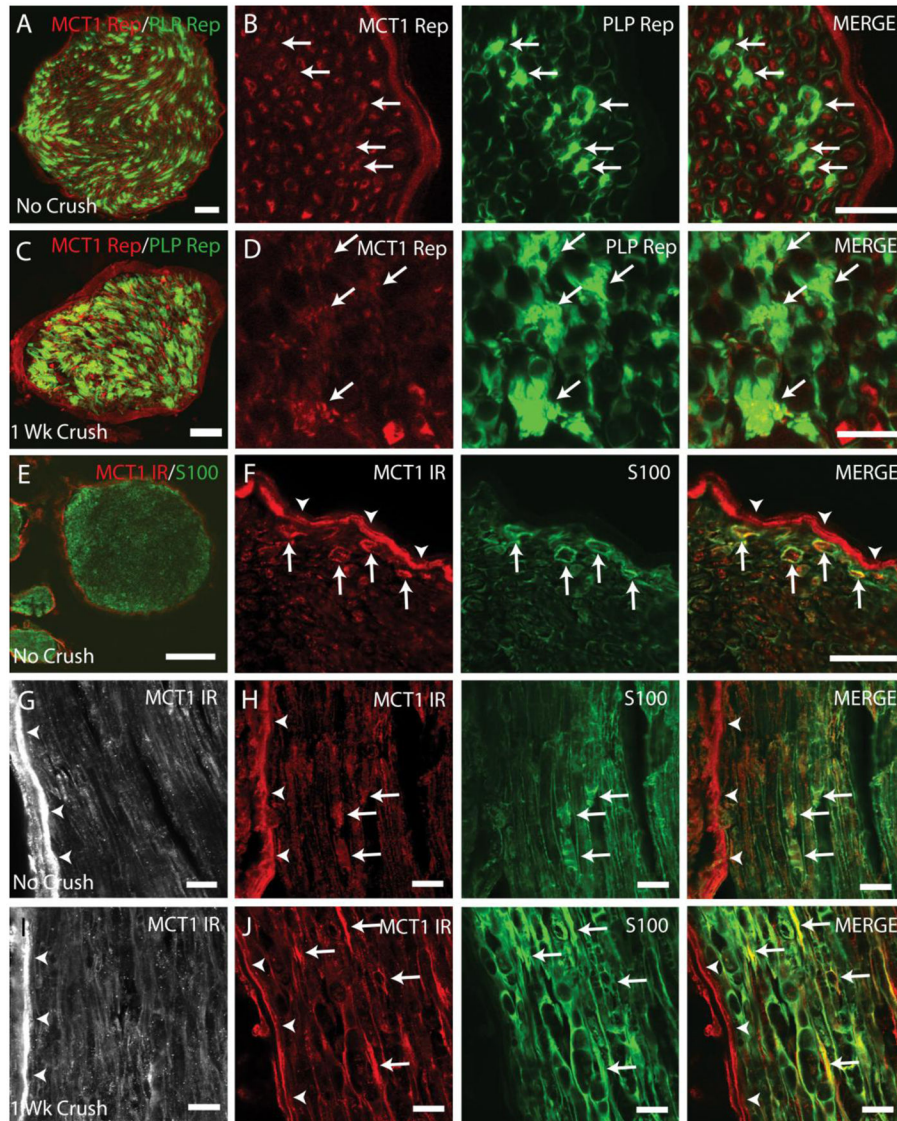


Figure 6. MCT1 is expressed by Schwann cells in intact and crushed peripheral nerves
 Cross-section of uncrushed (A, B) and 1 week crushed (C, D) sciatic nerves from MCT1 tdTomato and PLP-GFP double reporter transgenic mice (Scale bars A, C 50 μ m; scale bars B, D 20 μ m). Schwann cells expressing MCT1 (arrows) are indicated by co-localization of MCT1 reporter (MCT1 Rep; red) with PLP reporter (PLP Rep; green). Perineurium is indicated by arrowheads. Red fluorescence in MCT1 tdTomato reporter mice reflects mRNA gene expression within a given cell, but not specific transporter localization within the cell (i.e., dendrite versus axon or cell body). Uncrushed sciatic nerve from WT mice immunostained with MCT1 (red) and S100 (green) displayed in cross-section (E, F) and longitudinal (G, H) photomicrographs (Scale bar E 100 μ m; scale bar F–J 20 μ m). Sciatic nerves 1 week following crush (I, J) immunostained for MCT1 (red) and S100 (green). MCT1-immunoreactive profiles that co-localize with S100 (i.e., Schwann cells) are indicated by arrows and perineurium by arrowheads.

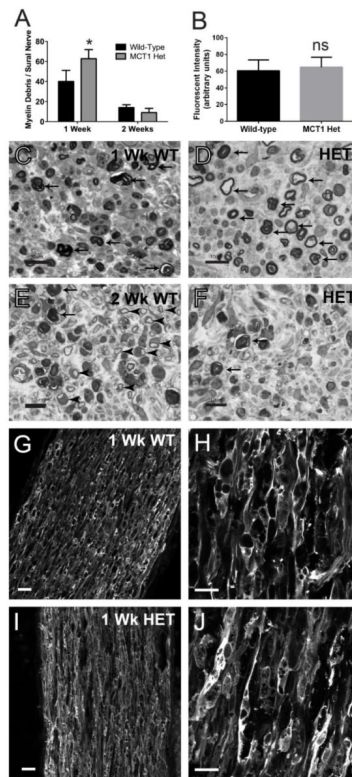


Figure 7. Myelin debris and macrophage infiltration in MCT1 heterozygous null (MCT1 Het) mice following sciatic nerve injury

The number of myelin debris per sural nerve fascicle (A) in WT and MCT1 Het mice are quantified at 1 and 2 weeks following sciatic nerve crush (n=4 at 1 week and n=2 at 2 weeks for each genotype). Mean MAC2 fluorescent intensity (B) in distal sciatic nerve from WT and MCT1 Het mice 1 week following sciatic nerve crush (N=4 of each genotype). Sural nerves from wild-type (WT; C, E) and MCT1 Het (D, F) mice 1 (C, D) or 2 (E, F) weeks following sciatic nerve crush (scale bars 20 μ m). Myelin debris is indicated by arrows and newly regenerated axons by arrowheads. Photomicrographs of MAC2 immunofluorescence in distal sciatic nerves 1 week following nerve crush in WT (G, H) and MCT1 Het (I, J) mice. All error bars reflect S.E.M. * p<0.05, ns non-significant

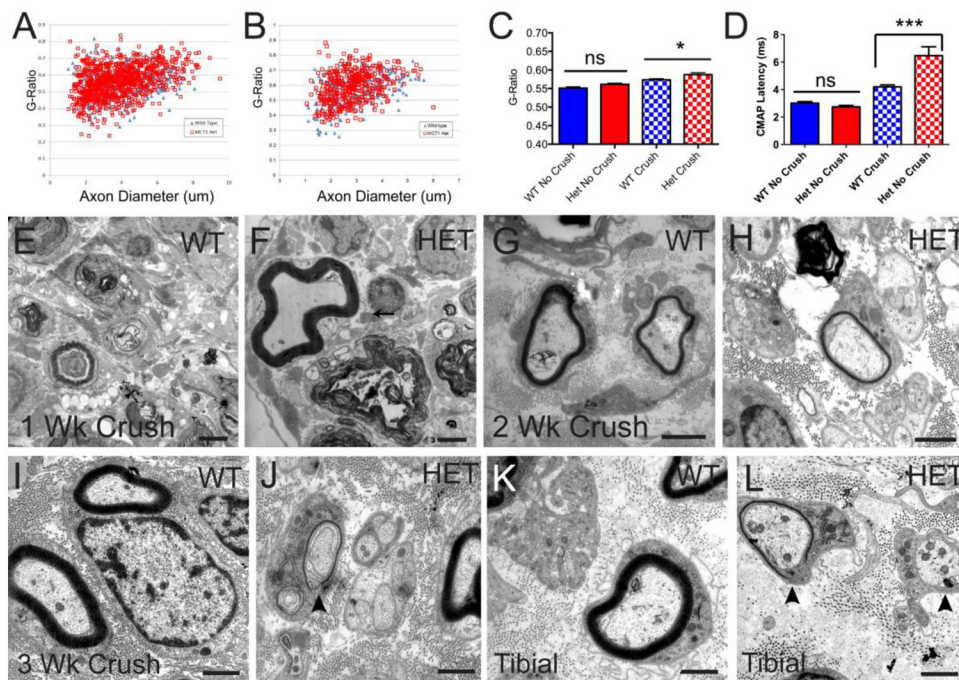


Figure 8. Regenerated peripheral nerves in MCT1 Het mice have delayed and incomplete remyelination

Uncrushed sural nerves from wild-type (WT; n=475 axons) and MCT1 Het (Het; n=964 axons) mice have identical G-ratios (A, C), while 6 week regenerated sural nerves from Het mice (n=770 axons) have significantly increased G-ratios compared to regenerated WT nerves (B, C; n=430 axons), reflecting thinner myelination. Electrophysiologically (D), the compound motor action potential (CMAP) latency from regenerating sciatic nerves from Het mice, but not uncrushed nerves, are prolonged compared to WT mice, reflecting reduced remyelination. Electron photomicrographs of sural nerves 1 weeks post-crush from WT (E) and Het (F) mice; 2 weeks post-crush from WT (G) and Het (H) mice; and 3 weeks post-crush from WT (I) and Het (J) mice, as well as from tibial nerves 3 weeks post-crush from WT (K) and Het (L) mice. An early myelin remnant is present in sural nerve from Het mice 1 week following sciatic nerve crush (F). Thinly myelinated or unmyelinated large axons (arrowheads) are seen in both sural (J) and tibial (L) nerves from MCT1 Het, but not WT (I, K), mice 3 weeks post-crush. Scale bars are all 2 μm. All error bars reflect S.E.M. * p<0.05, ns non-significant